Effective-parametric resonance in a non-oscillating system

Marcel G. Clerc, Claudio Falcón, Cristián Fernández-Oto and Enrique Tirapegui

Departamento de Física, Universidad de Chile - Casilla 487-3, Santiago, Chile

Abstract – We present a mechanism for the generation of oscillations and nonlinear parametric amplification in a non-oscillating system, which we term *effective-parametric resonance*. Sustained oscillations appear at a controlled amplitude and frequency, related directly to the external forcing parameters. We present an intuitive explanation for this phenomenon, based on an effective equation for a driven oscillation and discuss its relation to other approaches. More precisely, a high-frequency forcing can generate an effective oscillator, which may have a parametric resonance with the applied forcing. We point out the main ingredients for the development of effective-parametric resonance in non-oscillating systems and show its existence in a simple model. Theoretically, we calculate the appearance of this nonlinear oscillation by computing its stability curve, which is confirmed by numerical simulations and experimental studies on a vertically driven pendulum.

Introduction. – An oscillator displays resonances due to its ability to store and transfer energy coming from a forcing source into an internal oscillation mode, Galileo Galilei being one of the first to recognize them [1]. Resonance is at the core of physics, ranging from microscopic to macroscopic, from quantum to classical, and from deterministic to stochastic [2–4]. Resonances have been classified mainly in two different ways depending on the type of forcing acting on the oscillator. The most well-known type is characterized by the independence of the forcing from the oscillator state, which is termed as *resonance* [5]. The other type is known as *parametric resonance* [5]. The latter appears as an instability of a dissipative oscillatory system where one or more parameters are modulated in time or space, injecting energy into the system. As one of the control parameters of the system overcomes a certain threshold, a coherent oscillatory response develops with an amplitude that depends on the the nonlinear saturation of the instability. The oscillation frequency is given by a resonance condition relating injection and dissipation of energy with the mismatch between forcing and natural frequencies. It must be noticed that the idea of energy storing and transferring due to resonances can be even generalized to fluctuating systems [3].

In this work, we present a phenomenon arising from parametric amplification with revealing potential applications: the generation of *effective-parametric resonance* (EPR) which induces oscillations in a non-oscillating system, that is, a system that without parametric forcing cannot present permanent oscillations. The appearance of oscillations is known in the parametrically forced upside-down pendulum [6]. Parametric instabilities have been explained by the introduction of Mathieu functions. We present an alternative explanation allowing a simple interpretation, which can be intuitively extended to other physical contexts. We study EPR in a simple prototype model that allows us to build a description based on a forced system with an effective potential and apply these results to a parametrically amplified over-damped pendulum. In this simple system, we show theoretically, numerically, and experimentally the appearance of sustained oscillations with a given frequency and amplitude, controlled externally by the parametric forcing.

Prototype EPR system. – In order to characterize the EPR phenomenon, let us consider the following simple prototypical dynamical system:

$$\ddot{x} = -\gamma \sin(\omega t)x - \mu\dot{x} - \alpha x^3, \qquad (1)$$

where $x(t)$ is the variable that describes the state of the system, $\ddot{x}$ is the respective acceleration, μ is a viscous damping parameter accounting for energy dissipation, α characterizes the nonlinearity of the system, and γ and ω are, respectively, the intensity and frequency of the external parametric forcing. Other models can be chosen to describe the emergence of permanent oscillations by EPR; however, eq. (1) possesses the main ingredients necessary to describe this phenomenon.
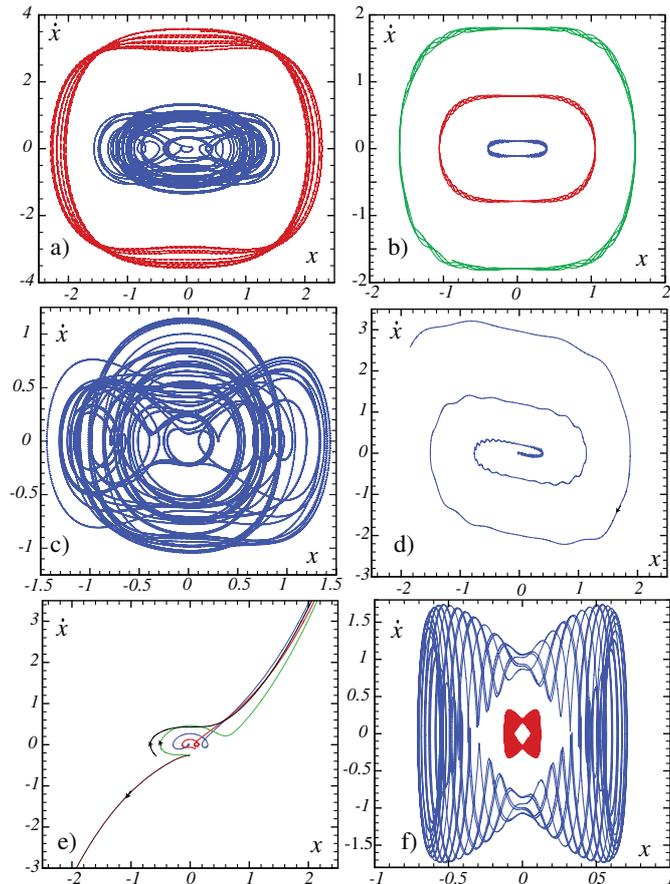
Fig. 1: (Color online) Phase portrait of model (1) for $\alpha = 1.0$, $\gamma = 1.0$, $\mu = 0$ and $\omega = 0.5$ a); $\alpha = 1.0$, $\gamma = 1.0$, $\mu = 0$ and $\omega = 20.0$ b); $\alpha = 1.0$, $\gamma = 1.0$, $\mu = 0.02$ and $\omega = 0.5$ c); $\alpha = 1.0$, $\gamma = 0.3$, $\mu = 0.2$ and $\omega = 10.0$ d); $\alpha = -2.0$, $\gamma = 46.5$, $\mu = 0.0$ and $\omega = 1.0$ e); $\alpha = -2.0$, $\gamma = 46.5$, $\mu = 0.0$ and $\omega = 20.0$ f).

To study the phenomenology of EPR, we have performed numerical simulations of model (1) using a fourth order Runge-Kutta algorithm with time step $\Delta t = 0.02$ for several values of the control parameters. In the non-dissipative limit ($\mu = 0$) for $\alpha > 0$, model (1) exhibits chaotic behavior near the origin and quasi-periodic behavior away from it when ω is of order 1, as illustrated in fig. 1a)). However, as ω increases sufficiently, the former scenario changes and the phase portrait described before is changed to the equivalent phase portrait of a simple oscillator, *i.e.*, chaotic behavior is transformed into quasi-periodic behavior (cf. fig. 1b)). In the dissipative regime ($\mu > 0$), the dynamics of the system is characterized by the appearance of a chaotic attractor [7], as depicted in fig. 1c). As ω increases sufficiently, the phase portrait displays the equivalent of a damped oscillator, as illustrated in fig. 1d). Even, the effect of large ω can even stabilize a non-oscillating system with divergent trajectories ($\alpha < 0$) with or without dissipation. Figure 1e) shows the phase portrait of model (1) for small ω displaying divergent trajectories. As ω increases, there is a qualitative change in the trajectories

as oscillations develop around the fixed point $x = \dot{x} = 0$ and trajectories do not diverge, as is shown in fig. 1f). Therefore, for large ω and γ of order 1, model (1) shows the emergence of oscillations.

Forced systems with explicit temporal dependence, as the one displayed in model (1), are usually studied in terms of first return maps using the time-dependent forcing period as the iteration period between two successive values of the map [8]. This approach will be of benefit in the case of low-frequency forcing, where the dominant time scale is the forcing scale. In the case of high-frequency forcing, first return maps describe basically the same dynamics as model (1). Furthermore, first return maps, although useful for calculations of stability of fixed points, and hence limit cycles, do not give an insight into the physical mechanism for the generation of the high-frequency dynamics explained above. Another way to study the high-frequency dynamics of eq. (1) that can present a way to interpret and understand the dynamics is the strategy proposed by Kapitza [9]: the previous high-frequency dynamics can be understood as a result caused by the separation of time scales between the forcing and the state variable $x(t)$ itself, which can explain the appearance of an effective force. Unlike the linear analysis based on Mathieu functions, this strategy allows a global description that contains the nonlinear response of the system. Therefore, a generalization of this type of strategy may allow us to glimpse into non-trivial phenomena arising from the original forced system. Following the strategy proposed by Kapitza, in the limit $\omega \gg \mu$, the dynamics is decomposed as

$$x(t) = z(t) + \frac{\gamma}{\omega^2}\sin(\omega t)z(t), \qquad (2)$$

where z accounts for the slow dynamics and the second term on the right-hand side stands for the small fast dynamics [9]. Introducing the above Ansatz in eq. (1), we obtain

$$\ddot{z} = -\frac{\gamma^2}{2\omega^2}z - \mu\dot{z} - \frac{2\gamma}{\omega}\cos(\omega t)\dot{z} - \frac{\gamma}{\omega^2}\sin(\omega t)\ddot{z}$$
$$+ \frac{\gamma^2}{2\omega^2}\cos(2\omega t)z - \frac{\mu\gamma}{\omega}\cos(\omega t)z - \frac{\mu\gamma}{\omega^2}\sin(\omega t)\dot{z}$$
$$- \alpha z^3\left[1 + \frac{\gamma}{\omega^2}\sin(\omega t)\right]^3. \qquad (3)$$

If one considers the limit, $\omega \gg 1$ and $\gamma/\omega^2 \ll 1$ averaging over a period $2\pi/\omega$, we obtain

$$\ddot{z} = -\gamma^2/2\omega^2 z - \alpha z^3 - \mu\dot{z}, \qquad (4)$$

which is the Kapitza dynamics. On the other hand, in the case of small z and considering that $\gamma/\omega^2 < 1$ but not small, the dominant order of eq. (3) takes the form

$$\ddot{z} = -\frac{\gamma^2}{2\omega^2}z - \alpha z^3 - \mu\dot{z} - \frac{2\gamma}{\omega}\cos(\omega t)\dot{z}, \qquad (5)$$

up to leading-order resonant terms in γ/ω. In this effective dynamical system $z(t)$ is a variable that accounts for
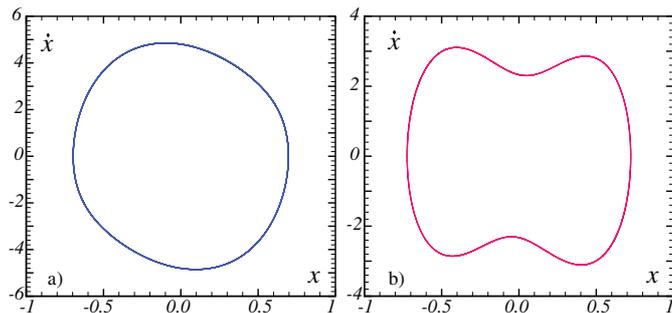
Fig. 2: (Color online) Phase portrait of prototype model (1) for $\alpha = 200.0$, $\gamma = 48.0$, $\mu = 1.0$ and $\omega = 14.0$ (a)) and $\alpha = -1.0$, $\gamma = 47.0$, $\mu = 1.0$ and $\omega = 10.0$ (b)).

slow dynamics of $x(t)$. The above model corresponds to an oscillator with an induced natural frequency $\omega_I \equiv \gamma/\sqrt{2}\omega$. In the limit of high frequencies ($\gamma \ll \omega^2$), the last term is neglected as a result of the separation of scales between $z(t)$ and the forcing, which corresponds to Kapitza analysis [5]. Hence, using this approach, the first term of the right-hand side is an effective force that leads the dynamics. Independently, if at moderate frequencies model (1) has divergent trajectories ($\alpha > 0$) or not ($\alpha < 0$), in the above limit the system can be described as an oscillator. Model (5) allows us to intuitively understand the dynamics exhibited by model (1) in this limit providing a way to understand the emergence of oscillations in non-oscillating systems submitted to high-frequency forcing. In brief, the non-oscillator system subjected to a high-frequencies forcing (eq. (1)) is equivalent to a parametrically driven oscillator with a well-defined natural frequency ($\gamma^2/2\omega^2$). Therefore, one expects intuitively that changing the value of the induced natural frequency one can observe the well-known characteristics of parametric resonance.

Appearance of EPR. For large but fixed ω, as we increase γ, the induced natural frequency increases. Furthermore, the terms neglected in the strategy of Kapitza grow in their amplitudes. The combination of these effects can generate the phenomenon of *effective-parametric resonance*: as ω_I approaches $\omega/2$ and the forcing and dissipative terms can be balanced, the system can resonate by parametrically amplifying itself. Hence, by modifying γ appropriately, the system can display this phenomenon when $\gamma \sim \sqrt{2}\omega^2/2$. Therefore, $x = \dot{x} = 0$ becomes unstable and nonlinearity saturates this instability leading to attractive periodic solutions. Figures 2a) and b) show the stable limit cycle generated by EPR for both positive and negative α. Thus, for large ω and γ which satisfy the above resonance condition, model (1) induces simultaneously a natural frequency of oscillation and a parametric forcing, giving rise to effective-parametric resonance at half the forcing frequency even for large dissipation. From these simulations, we can infer that in the case of positive (negative) α, the observed limit cycle is dominated by the first dominant mode (first two
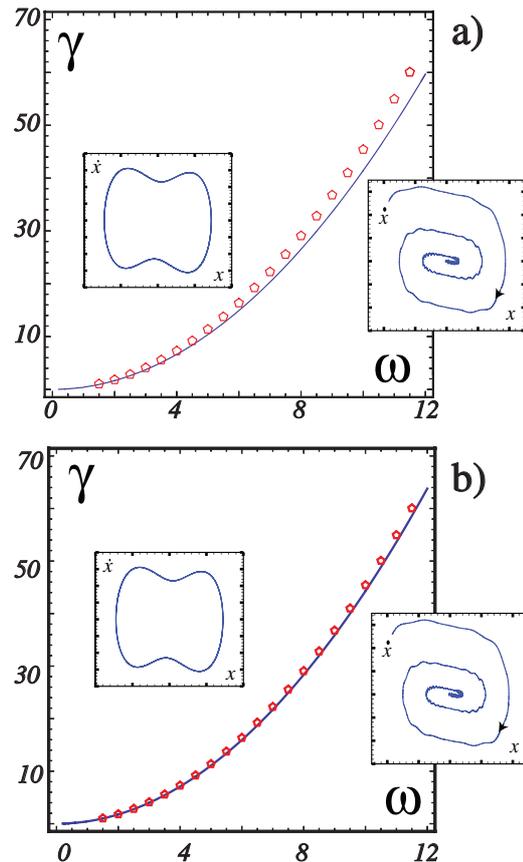

Fig. 3: (Color online) Effective-parametric resonance curve in γ-ω space for $\mu = 0.1$ and $\alpha = -1.0$. Above the line, the system shows effective-parametric resonance. Pentagon symbols are obtained by numerical simulation of model (1). The solid line in a) and b) is, respectively, deduced from models (5) and (3). Left insets: limit cycle. Right insets: damped oscillations towards $x = 0$.

dominant modes). This explains the different limit cycles in the x-$\dot{x}$ phase portrait displayed in fig. 2.

We perform a modal expansion for eq. (5) and, keeping the dominant terms of modal expansion up to order γ/ω, one finds the curve $(\gamma/2\omega)^2 = (\mu/2)^2 + (\omega/2 - \gamma/\omega\sqrt{2})^2$ for the stability of $x = 0$. To corroborate this prediction we have performed numerical simulations of model (1) in the ω-γ space, showing good agreement with the predicted curve. In fig. 3a) we show both theoretical and numerical results. On the other hand, using the same modal expansion in eq. (3) allows us compute an amended instability curve, which improves the accuracy to within 3% from the previous expression as is shown in fig. 3b), although the qualitative shape of the curve is the same. Thus, our first-order approximation agrees consistently with numerical simulations of the instability curve. Above the curve a stable limit cycle in the x-$\dot{x}$ phase portrait develops (fig. 3, left inset), whereas outside of it damped oscillations towards $x = \dot{x} = 0$ appear (fig. 3, right inset). In the case of $\alpha < 0$, for small (large) μ compared with ω, effective-parametric

resonance develops as a super(sub)-critical instability, that is, when one increases γ the system shows the appearance of a infinitesimal (finite) limit cycle. In the other case ($\alpha > 0$), one observes the opposite behavior.

EPR in a vertically driven pendulum. – As we have noted before, EPR results from the effect of the parametric amplification of a system by a large-amplitude and high-frequency forcing. As mentioned above, a simple mechanical system that shows this effect is a vertically driven pendulum. The upside-down state becomes stable at high frequencies even for small displacement amplitudes of the support point, as a result of the emergence of an oscillator where the upside-down position is a stable fixed point [5]. This counterintuitive fact was first predicted analytically in the pioneering work of Stephenson [10] which spanned a large ammount of theoretical [5] and experimental discussions [11,12] of the phenomenon. As the displacement amplitude is increased, it was observed numerically [13] and experimentally [12] the appearance of a nonlinearly saturated oscillation around the upside-down position. This is a limit cycle in the ϕ-$\dot\phi$ phase portrait, where ϕ is the angle of the pendulum with respect to the vertical axis and $\dot\phi$ is the angular velocity. This phenomenon was associated with a Hopf bifurcation [7], which is related to a time-independent linear operator. This statement is inadequate for the upside-down position because the linear stability analysis of this state is related to a periodic time-dependent linear operator which requires the use of Floquet theory [14]. On the other hand, this behavior can be inferred as a consequence of the linear analysis based on Mathieu functions for negligible dissipation showing that the upside-down state is unstable. Alternatively, using a weakly nonlinear analysis, one finds that the dynamics around the upside-down state is similar to model (1) with negative α. Therefore, the appearance of permanent oscillations with respect to the vertical state is the result of EPR. It is important to note that in the study of the Faraday instability for strong viscous fluid a similar resonant condition is established in ref. [15].

Experimental study. A parametrically excited pendulum is built to explore EPR. A stainless-steel cylindrical roller bearing (internal diameter 8 mm, external diameter 15 mm) is mounted vertically into a plexiglass plate ($10 \times 15 \times 4$ mm^3), see fig. 4. A plexiglass cylinder is fixed solidary to a cylindrical roller bearing, which enables it to rotate smoothly in a plane. A massive bronze bar (length 60 mm, diameter 3 mm) is eccentrically positioned 2 mm from the center of the cylinder (cf. fig. 4), displacing the center of mass from the center of the plexiglass cylinder. This asymmetry generates a physical pendulum with a natural frequency $f_0 \approx 10$ Hz ($\omega_0 \approx 30$ ad/s) and oscillating radius $l \approx 2$ mm. The whole system is then mounted over an electromechanical shaker driven sinusoidally by a frequency generator via a power amplifier. The modulation of the acceleration of gravity $a_{ex}\omega_{ex}^2\cos(\omega_{ex}t)$ with $\omega_{ex} = 2\pi f_{ex}$ is measured directly by a piezoelectric
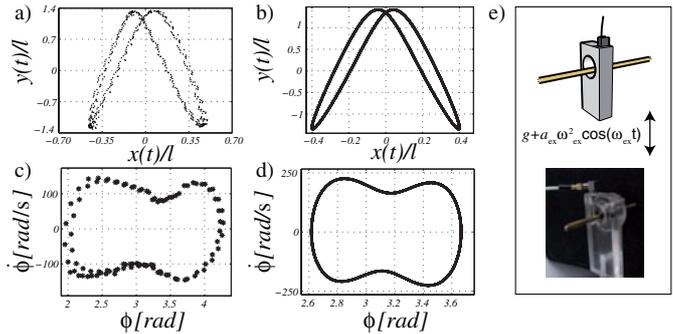

Fig. 4: A Lissajous figure of the nonlinear oscillations around the inverted pendulum position is obtained experimentally (a)) and numerically (b)). The limit cycle oscillating around the inverted position of a physical pendulum is found experimentally (c)) and numerically (d)). e) Schematic representation and snapshot of the physical pendulum under consideration.

accelerometer and a charge amplifier. The control parameters are then ω_{ex} and a_{ex} ($\gamma_{ex} = a_{ex}\omega_{ex}^2/l$). The motion of the pendulum is acquired with a high-speed camera at 500 fps in a 800×600 pixel window.

We explore the large-frequency limit $\omega_{ex}/\omega_0 \gg 1$ in the particular case of $a_{ex}/l \sim 1$, which corresponds $\gamma_{ex} \sim \omega_{ex}^2$. For a given ω_{ex}, by increasing the amplitude of modulation a_{ex} the inverted pendulum is stabilized. As a_{ex} continues to increase, new equilibria appear, namely a limit cycle, which oscillates at $f_{ex}/2$ around the inverted position $\phi = \pi$. This type of limit cycle also appears oscillating around $\phi = 0$. These oscillations cannot occur in the unforced system, due to its highly dissipative nature. In fig. 4a), we show a typical trajectory of the center of mass of the pendulum found experimentally for $\omega_{ex}/\omega_0 \approx 5$ and $a_{ex}/l \approx 2$, and in fig. 4b) the numerically computed trajectory. They display Lissajous figures with two frequencies, one being f_{ex} and the other one being $f_{ex}/2$. We also show in figs. 4c) and d) the phase portrait. Notice that the limit cycle is surrounding the inverted position $\phi = \pi$.

Conclusions. – The usual strategy to induce oscillations is done by exciting the natural frequencies (or entire multiples of these frequencies) of a system under study. We show here that the use of high-frequency forcing —the forcing periods are smaller than any characteristic time scale of the system under study in non-oscillating systems— can induce an effective natural frequency of oscillation and simultaneously induce parametric amplification through resonance even for large dissipation. Both effects are responsible for the appearance of permanent oscillations. We have considered a simplest model, eq. (1), to illustrate these behaviors. Analytically based on a generalization of the strategy proposed by Kapitza, we have succeeded in explaining this effective-parametric resonance. However, the obtained results are quite general. It suffices to consider a system of at least two variables

forced parametrically at high frequencies, which can induce an effective oscillator and that in a suitable parameter region can exhibit effective-parametric resonance. Recent studies showed that the shape of the forcing, contrary to common wisdom, can qualitatively change the scenario of the expected dynamic behavior [16,17]. Theoretical, numerical and experimental studies on effective-parametric resonance for non-harmonic forcing are currently in progress.

$$* * *$$

REFERENCES

[1] FROVA A. and MARENZANA M., *Thus Spoke Galileo: The Great Scientist's Ideas and their Relevance to the Present Day* (Oxford University Press) 2006.
[2] FRENCH A. P., *Vibrations and Waves (The M.I.T. Introductory Physics Series)* (W. W. Norton & Company) 1971; BUZSÁKI G., *Rhythms of the Brain* (Oxford University Press) 2006.
[3] GAMMAITONI L., HANGGI P., JUNG P. and MARCHESONI F., *Rev. Mod. Phys.*, **70** (1998) 223.
[4] ANDRONOV A. A. and CHAIKIN C. E., *Theory of Oscillations* (Princeton University Press) 1949.
[5] LANDAU L. D. and LIFSHIFTZ E. M., *Mechanics,* Vol. **1** *(Course of Theoretical Physics)* (Pergamon Press) 1976.
[6] MCLACHLAN N. W., *Theory and Application of Mathieu Functions* (Oxford University Press) 1951.
[7] JACKSON A., *Perspectives of Nonlinear Dynamics*, Vol. **2** (Cambridge University Press) 1960.
[8] OTT E., *Chaos in Dynamical Systems* (Cambridge University Press) 2002.
[9] KAPITZA P. L., *Sov. Phys. JETP*, **21** (1951) 588; *in Collected Papers of P. L. Kapitza*, edited by TER HAAR D. (Pergamon Press) 1965.
[10] STEPHENSON A., *Philos. Mag.*, **15** (1908) 233; *Mem. Proc. Manch. Lit. Phil. Soc.*, **52** (1908) 1.
[11] KALMUS H. P., *Am. J. Phys.*, **38** (1970) 874; MICHAELIS M. M., *Am. J. Phys.*, **53** (1985) 1079; FRIEDMAN M. H., CAMPANA J. E. and YERGEY A. L., *Am. J. Phys.*, **50** (1982) 924.
[12] SMITH H. J. T. and BLACKBURN J. A., *Am. J. Phys.*, **60** (1992) 909.
[13] BLACKBURN J. A., SMITH H. J. T. and GRØNBECH-JENSEN N., *Am. J. Phys.*, **60** (1992) 903.
[14] HALE J. K., *Ordinary Differential Equations* (John Wiley & Sons) 1969.
[15] CERDA E. A. and TIRAPEGUI E. L., *Phys. Rev. Lett.*, **78** (1997) 859; *J. Fluid Mech.*, **368** (1998) 368.
[16] WEI M. D. and HSU C. C., *Opt. Commun.*, **285** (2012) 1366.
[17] CHACON R., ULEYSKY M. Y. and MAKAROV D. V., *EPL*, **90** (2010) 40003.